3. Elastic Scattering from Many-Body Systems

Thomas Brückel, IFF, FZ-Jülich

3.1 Introduction

So far we have learnt about the production of neutrons and their interaction with a single atom. In this chapter, we will discuss the scattering of thermal neutrons from a sample containing many atoms. In the first part, we will assume that the atoms are non-magnetic and only the scattering from the nucleus will be considered. In the second part, we will discuss the scattering from the spin- and orbital- angular momentum of the electrons in a magnetic solid.

For simplification, we will assume in this chapter that the atoms are rigidly fixed on equilibrium positions, i. e. they are not able to absorb recoil energy. This assumption is certainly no longer valid, if the neutrons are scattered from a gas, especially in the case of hydrogen, where neutron and the atom have nearly the same mass. In this case, the neutron will change its velocity, respectively its energy, during the scattering event. This is just the process of moderation and without this so-called inelastic scattering (i. e. scattering connected with a change of kinetic energy of the neutron) we would not have thermal neutrons at all. Also when scattered from a solid (glass, polycrystalline or single crystalline material) neutrons can change their velocity for example by creating sound waves (phonons). However, in the case of scattering from a solid, there are always processes in which the recoil energy is being transferred to the sample as a whole, so that the neutron energy change is negligible and the scattering process appears to be elastic. In this chapter we will restrict ourselves to only these scattering processes, during which the energy of the neutron is not changed. In subsequent chapters, we will learn how large the fraction of these elastic scattering processes is, as compared to all scattering processes.

Quantum mechanics tells us that the representation of a neutron by a particle wave field enables us to describe interference effects during scattering. A sketch of the scattering process in the so-called *Fraunhofer* approximation is given in figure 3.1.

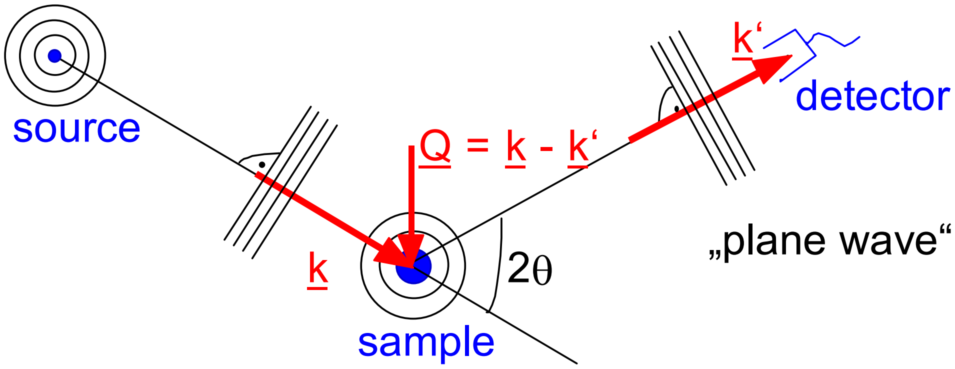

Fig. 3.1: A sketch of the scattering process in the Fraunhofer approximation, in which it is assumed that plane waves are incident on sample and detector due to the fact that the distance source-sample and sample-detector, respectively, is significantly larger than the size of the sample.

In the Fraunhofer approximation it is assumed that the size of the sample is much smaller than the distance between sample and source and the distance between sample and detector, respectively. This assumption holds in most cases for neutron scattering experiments. Then the wave field incident on the sample can be described as plane waves. We will further assume that the source emits neutrons of one given energy. In a real experiment, a so-called *monochromator* will select a certain energy from the white reactor spectrum. Altogether, this means that the incident wave can be completely described by a wave vector $\underline{k}$. The same holds for the wave incident on the detector, which can be described by a vector $\underline{k}'$. In the case of elastic scattering (diffraction), we have:

$$k = |\underline{k}| = |\underline{k}'| = k' = \frac{2\pi}{\lambda} \tag{3.1}$$

Let us define a so-called *scattering vector* by:

$$\boxed{\underline{Q} = \underline{k} - \underline{k}'} \tag{3.2}$$

The magnitude of the scattering vector can be calculated from wave length λ and scattering angle 2θ as follows:

$$Q = \left|\underline{Q}\right| = \sqrt{k^2 + k'^2 - 2kk'\cos 2\theta}$$

$$\Rightarrow \boxed{Q = \frac{4\pi}{\lambda}\sin\theta} \tag{3.3}$$

During a scattering experiment, the intensity distribution is being determined as a function of the scattering vector:

$$I \sim \frac{d\sigma}{d\Omega}\left(\underline{Q}\right) \tag{3.4}$$

The proportionality factors arise from the detailed geometry of the experiment. Our task is to determine the arrangement of the atoms in the sample from the knowledge of the scattering cross section $d\sigma/d\Omega(\underline{Q})$. The relationship between scattered intensity and the structure of the sample is especially simple in the approximation of the so-called *kinematic scattering*. In this case, multiple scattering events and the extinction of the primary beam due to scattering in the sample are being neglected. Following figure 3.2, the phase difference between a wave scattered at the origin of the co-ordinate system and at the position $\underline{r}$ is given by:

$$\underline{k} \cdot \underline{r} - \underline{k}' \cdot \underline{r} = \underline{Q} \cdot \underline{r} \tag{3.5}$$

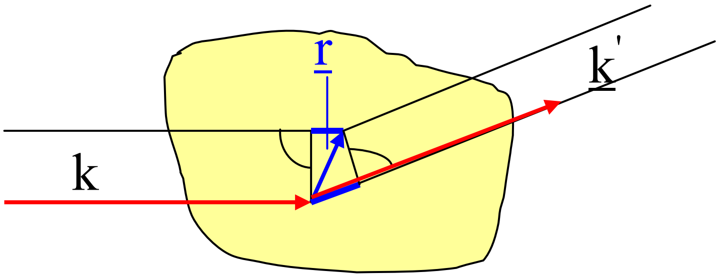

Fig. 3.2: A sketch illustrating the phase difference between a beam being scattered at the origin of the co-ordinate system and a beam scattered at the position $\underline{r}$.

The scattered amplitude at the position $\underline{r}$ is proportional to the *scattering power density* $\rho_S\left(\underline{r}\right)$. The meaning of ρ_s in the case of neutron scattering will be given later. The total scattered amplitude is given by a coherent superposition of the scattering from all positions $\underline{r}$ within the sample, i. e. by the integral:

$$A = \int \rho_S(\underline{r}) \cdot e^{i\underline{Q}\cdot\underline{r}} d^3 r \qquad (3.6)$$

I.e. the scattered amplitude is connected with the scattering power density $\rho_S(\underline{r})$ by a simple Fourier transform:

$$A = F(\rho_S(\underline{r})) \qquad (3.7)$$

A knowledge of the scattering amplitude for all scattering vectors $\underline{Q}$ allows us to determine via a Fourier transform the scattering power density uniquely. This is the complete information on the sample, which can be obtained by the scattering experiment. Unfortunately, life is not so simple. There is the more technical problem that one is unable to determine the scattering cross section for <u>all</u> values of $\underline{Q}$. The more fundamental problem, however, is given the fact that normally the amplitude of the scattered wave is not measurable. Instead only the scattered intensity $I \sim |A|^2$ can be determined. Therefore, the phase information is lost and the simple reconstruction of the scattering power density via a Fourier transform is no longer possible. This is the so-called *phase problem* of scattering.

The question what we can learn about the structure of the sample from a scattering experiment despite this problem will be the subject of the following chapters. For the moment, we will ask ourselves the question, which wavelength we have to choose to achieve atomic resolution. The distance between neighbouring atoms is in the order of a few times 0.1 nm. In the following we will use the “natural atomic length unit” 1 Å = 0.1 nm. To obtain information on this length scale, a phase difference of about $Q \cdot a \approx 2\pi$ has to be achieved, compare (3.5). According to (3.3) $Q \approx \frac{2\pi}{\lambda}$ for typical scattering angles ($2\theta \approx 60°$). Combining these two estimations, we end up with the requirement that the wavelength λ has to be in the order of the inter-atomic distances, i. e. in the order of 1 Å to achieve atomic resolution in a scattering experiment. This condition is ideally fulfilled for thermal neutrons.

3.2 Fundamental Scattering Theory

In this chapter, we will give a simple formulation of scattering theory. Our purpose is to derive (3.7) from fundamental principles. The conditions under which (3.7) holds and the limitations of kinematical scattering theory will thus become clearer. During a first reading this section can be skipped. More details can be found in [1].

In quantum mechanics, neutrons are described as particle wave fields through the Schrödinger equation:

$$H\Psi = \left(-\frac{\hbar^2}{2m_n}\Delta + V \right)\Psi = i\hbar\frac{\partial}{\partial t}\Psi \tag{3.8}$$

ψ is the probability density amplitude, V the interaction potential. In the case of purely elastic scattering E = E', the time dependence can be described by the factor $\exp\left(-i\frac{E}{\hbar}t \right)$. Assuming this time dependence, a wave equation for the spatial part of the probability density amplitude ψ can be derived from (3.8):

$$\Delta\Psi + k^2(\underline{r})\Psi = 0 \tag{3.9}$$

In (3.9) we have introduced a spatially varying wave vector with the magnitude square:

$$k^2(\underline{r}) = \frac{2m_n}{\hbar^2}(E - V(\underline{r})) \tag{3.10}$$

Solutions of (3.8) in empty space can be guessed immediately. They are given by plane waves $\Psi = \Psi_0 \exp\left[i\left(\underline{k}\cdot\underline{r} - \frac{E}{\hbar}t \right) \right]$ with $k^2 = \frac{2m_n}{\hbar^2}E$. The relations between magnitude of the wave vector, wave length and energy of the neutron E can be written in practical units:

$$\boxed{\begin{aligned} &k\left[\mathring{A}^{-1}\right] \approx 0.695\sqrt{E\left[meV\right]} \\ &\lambda\left[\mathring{A}\right] \approx 9.045/\sqrt{E\left[meV\right]} \\ &E\left[meV\right] \approx 81.8/\lambda^2\left[\mathring{A}\right] \end{aligned}} \tag{3.11}$$

To give an example, neutrons of wavelength $\lambda = 2.4$ Å have an energy of 14.2 meV with a magnitude of the neutron wave vector of $k = 2.6$ Å^{-1}.

To obtain solutions of the wave equation (3.9) in matter, we reformulate the differential equation by explicitly separating the interaction term:

$$\left(\Delta + k^2\right)\Psi = \frac{2m_n}{\hbar^2} V \cdot \Psi =: \chi \tag{3.12}$$

Here $\underline{k}$ denotes the wave vector for propagation in empty space. The advantage of this formulation is that the solution of the left hand side are already known. They are the plane waves in empty space. Equation (3.12) is a linear partial differential equation, i. e. the superposition principle holds: the general solution can be obtained as a linear combination of a complete set of solution functions. The coefficients in the series are determined by the boundary conditions. To solve (3.12) one can apply a method developed for inhomogeneous linear differential equations. For the moment, we assume that the right hand side is fixed (given as χ). We define a "*Greens-function*" by:

$$\left(\Delta + k^2\right)G\left(\underline{r}, \underline{r}'\right) = \delta\left(\underline{r} - \underline{r}'\right) \tag{3.13}$$

We can easily verify that a solution of (3.13) is given by:

$$G\left(\underline{r}, \underline{r}'\right) = \frac{e^{ik\left|\underline{r} - \underline{r}'\right|}}{4\pi\left|\underline{r} - \underline{r}'\right|} \tag{3.14}$$

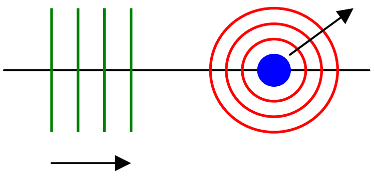

The meaning of (3.14) is immediately clear: the scattering from a point-like scatterer (δ-potential) gives a emitted spherical wave.

Using the "Greens-function" G($\underline{r}$,$\underline{r}$'), a formal solution of the wave equation (3.12) can be given:

$$\Psi = \Psi^{o} + \int G(\underline{r},\underline{r}')\chi(\underline{r}')d^{3}r' \tag{3.15}$$

Here, we have taken the initial conditions of a incident plane wave ψ^0 into account. That (3.15) is indeed a solution of (3.12) can be easily verified by substituting (3.15) into (3.12). If we finally substitute the definition of χ, one obtains:

$$\Psi(\underline{r}) = \psi^{o}(\underline{r}) + \frac{2m_n}{\hbar^2}\int G(\underline{r},\underline{r}')V(\underline{r}')\Psi(\underline{r}')d^{3}r' \tag{3.16}$$

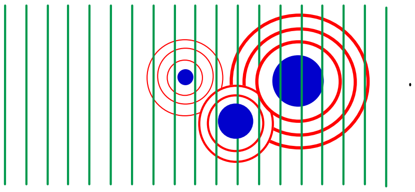

(3.16) has a simple interpretation: the incident plane wave $\psi^0(\underline{r})$ is superimposed by spherical waves emitted from scattering at positions $\underline{r}$'. The intensity of these spherical waves is proportional to the interaction potential V($\underline{r}$') and the amplitude of the wave field at the position $\underline{r}$'. To obtain the total scattering amplitude, we have to integrate over the entire sample volume.

However, we still have not solved (3.12): our solution ψ appears again in the integral in (3.16). In other words, we have transformed differential equation (3.12) into an integral equation. The advantage is that for such an integral equation, a solution can be found by iteration. In the zeroth approximation, we neglect the interaction V completely. This gives $\psi = \psi^0$. The next higher approximation for a weak interaction potential is obtained by substituting this solution in the right hand side of (3.16). The first non-trivial approximation can thus be obtained:

$$\Psi^1(\underline{r}) = e^{i\underline{k}\cdot\underline{r}} + \frac{2m_n}{\hbar^2}\int \frac{\exp\left(ik\left|\underline{r}-\underline{r}'\right|\right)}{4\pi\left|\underline{r}-\underline{r}'\right|} V(\underline{r}')e^{i\underline{k}\underline{r}'}d^3r' \qquad (3.17)$$

(3.17) is nothing else but a mathematical formulation of the well-known *Huygens principle* for wave propagation.

The approximation (3.17) assumes that the incident plane wave is only scattered once from the potential $V(\underline{r}')$. For a stronger potential and larger sample, multiple scattering processes can occur. Again, this can be deduced from the integral equation (3.16) by further iteration. For simplification we introduce a new version of equation (3.16) by writing the integral over the "Greens function" as operator **G**:

$$\psi = \psi^o + \mathbf{G}V\psi \qquad (3.18)$$

The so-called *first Born approximation*, which gives the *kinematical scattering theory* is obtained by substituting the wave function ψ on the right hand side by ψ^0:

$$\psi^1 = \psi^o + \mathbf{G}V\psi^o \qquad (3.19)$$

This first approximation can be represented by a simple diagram as a sum of an incident plane wave and a wave scattered once from the potential V.

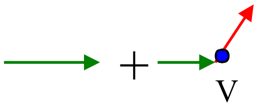

The second approximation is obtained by substituting the solution of the first approximation (3.19) on the right hand side of equation (3.18):

$$\begin{aligned}\psi^2 &= \psi^o + \mathbf{G}V\psi^1\\ &= \psi^o + \mathbf{G}V\psi^o + \mathbf{G}V\mathbf{G}V\psi^o \qquad (3.20)\end{aligned}$$

Or in a diagrammatic form:

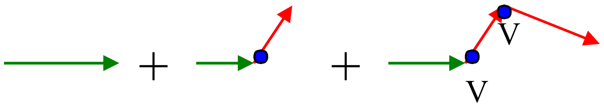

I. e. in the second approximation, processes are being taken into account, in which the neutron is scattered twice by the interaction potential V. In a similar manner, all higher order approximations can be calculated. This gives the so-called *Born series*. For a weak potential and small samples, this series converges rather fast. Often, the first approximation, the kinematic scattering theory, holds very well. This is especially the case for neutron scattering, where the scattering potential is rather weak, as compared to x-ray- or electron- scattering. Due to the strong Coulomb interaction potential, the probability for multiple scattering processes of electrons in solids is extremely high, making the interpretation of electron diffraction experiments very difficult. But even for neutrons, the kinematic scattering theory can break down, for example in the case of Bragg scattering from large ideally perfect single crystals, where the Born series does not converge. The wave equation has to be solved exactly under the boundary conditions given by the crystal geometry. For simple geometries, analytical solutions can be obtained. This is then called the *dynamical scattering theory*. Since for neutrons, the kinematical theory holds in most cases, or multiple scattering events can be corrected for easily, we will no longer discuss dynamical theory in what follows and refer to [1, 2].

Let us return to the first Born approximation (3.17). According to Fraunhofer, we assume in a further approximation that the size of the sample is significantly smaller than the distance sample-detector. The geometry to calculate the far field limit of (3.17) is given in figure 3.3.

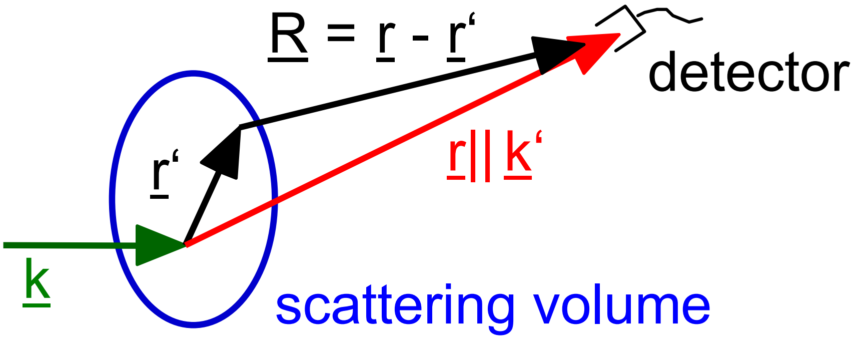

Fig. 3.3: Scattering geometry for the calculation of the far field limit at the detector. In the Fraunhofer approximation, we assume that $|\underline{R}| >> |\underline{r}'|$.

Under the assumption $|\underline{R}| >> |\underline{r}'|$, we can deduce from figure 3.3 the following approximation for the emitted spherical wave:

$$\frac{\exp\left(ik|\underline{r}-\underline{r}'|\right)}{|\underline{r}-\underline{r}'|} \approx \frac{\exp\left(ik\left(R-\underline{r}'\cdot\hat{\underline{R}}\right)\right)}{R} \approx \frac{\exp ikR}{R}\cdot e^{-i\underline{k}'\cdot\underline{r}'} \qquad (3.21)$$

The probability density amplitude for the scattered wave field in the limit of large distances from the sample is thus given by:

$$\Rightarrow \psi^1(\underline{R}) = e^{i\underline{k}\cdot\underline{R}} + \frac{2m_n}{\hbar^2}\frac{e^{ikR}}{4\pi R}\int V(\underline{r}')e^{i\underline{Q}\cdot\underline{r}'}d^3r' \qquad (3.22)$$

This is just the sum of an incident plane wave and a spherical wave emitted from the sample as a whole. The amplitude of the scattered wave is given according to (3.22):

$$\boxed{\begin{aligned} A(\underline{Q}) &= \frac{2m_n}{4\pi\hbar^2}\int V(\underline{r})e^{i\underline{Q}\cdot\underline{r}}d^3r \\ &\sim F[V(\underline{r})] \end{aligned}} \qquad (3.23)$$

I. e. the amplitude of the scattered wave is proportional to the Fourier transform of the interaction potential in the sample. In the case of pure nuclear scattering of neutrons, this interaction potential is the *Fermi-pseudo-potential* (see proceeding chapter). Finally, the measured intensity is proportional to the magnitude square of the scattering amplitude:

$$I(\underline{Q}) \sim |A(\underline{Q})|^2 \qquad (3.24)$$

3.3 The Patterson- or Pair-Correlation-Function

As already mentioned in the introduction, the phase information is lost during the measurement of the intensity according to (3.24). For this reason, the Fourier transform of the scattering potential is not directly accessible in most scattering experiments (note, however that phase information can be obtained in certain cases). In this section, we will discuss, which information can be obtained from the intensity distribution of a scattering experiment.

The same problem will be dealt with in a more general context in the chapter on correlation functions. Substituting (3.23) into (3.24), we obtain for the magnitude square of the scattering amplitude, a quantity directly accessible in a scattering experiment:

$$
\begin{aligned}
|A(\underline{Q})|^2 \Big/ \left(\frac{2m_n}{4\pi\hbar^2}\right)^2 &= \int V(\underline{r}) e^{i\underline{Q}\cdot\underline{r}} d^3r \int V^*(\underline{r}') e^{-i\underline{Q}\cdot\underline{r}'} d^3r' \\
&= \iint d^3r d^3r' V(\underline{r}) V^*(\underline{r}') e^{i\underline{Q}(\underline{r}-\underline{r}')} \\
&= \underset{\underset{\underline{r}-\underline{r}'=:\underline{R}}{\uparrow}}{} \int \mathrm{d}^3\mathrm{R} \int \mathrm{d}^3\mathrm{r} \mathrm{V}(\underline{\mathrm{R}}+\underline{\mathrm{r}}) \mathrm{V}^*(\underline{\mathrm{r}}) e^{\mathrm{i}\underline{\mathrm{Q}}\cdot\underline{\mathrm{r}}}
\end{aligned}
$$

This shows that the scattered intensity is proportional to the Fourier transform of a function P(R):

$$
I(\underline{Q}) \sim |A(\underline{Q})|^2 \sim F_{\underline{R}}[P(\underline{R})] \qquad (3.25)
$$

However, this function is not the interaction potential, but the so-called *Patterson-function:*

$$
\boxed{P(\underline{R}) = \int d^3r V^*(\underline{r}) V(\underline{r}+\underline{R})} \qquad (3.26)
$$

This function correlates the value of the interaction potential at position r, with the value at the position r + R, integrated over the entire sample. If, averaged over the sample, no correlation exists between the values of the interaction potential at position R and r + R, then the Patterson function P(R) vanishes. If, however, a periodic arrangement of a pair of atoms exists in the sample with a difference vector for the positions R, then the Patterson function will have an extremum for this vector R. Thus, the Patterson function reproduces all the vectors connecting one atom with an other atom in a periodic arrangement. In fact, the Patterson function is just a special case of the pair correlation functions accessible by scattering.

The meaning of the Patterson function can be illustrated by a simple example. Figure 3.4 shows an arrangement of three atoms in the form of a triangle. We can construct the Patterson function by copying this original pattern and shifting the copy with respect to the original by a difference vector R. In this case of a discrete distribution of the interaction potential V(r) (we also assume that V(r) is real), we can just count how many points of the original and the translated pattern coincide for this given difference vector R. Only if two or more atoms coincide, will we have a non-vanishing value for P(R) according to (3.26) for this discrete distribution of potentials. In this manner we can construct the Patterson function given in figure 3.4.

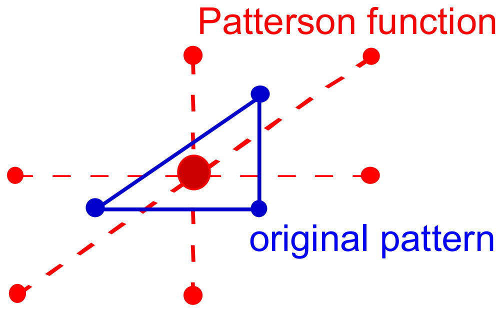

Fig. 3.4: Construction of the Patterson function for a pattern, which consists of three atoms at the corners of a triangle.

It is this function which we would obtain by Fourier transforming the diffraction pattern of a periodic arrangement of our original triangular pattern. One can easily see that in the Patterson function all vectors connecting one atom with any other one in the original pattern can be obtained. In our simple case, the original pattern can be guessed. However, the guess is not unique: we could also choose the mirror image.

3.4 Scattering from a Periodic Lattice in three Dimensions

As an example for the application of formulas (3.23) and (3.24), we will now discuss the scattering of thermal neutrons from a single crystal. More precisely, we will restrict ourselves to the case of a Bravais lattice with one atom at the origin of the unit cell. We further assume that there is only one isotope with scattering length b. The single crystal is finite with N-, M- and P-periods along the basis vectors a, b and c. The scattering potential, which we have to use in (3.23) is a sum over the Fermi-pseudo-potentials of all atoms:

$$V(\underline{r}) = \sum_{n=0}^{N-1} \sum_{m=0}^{M-1} \sum_{p=0}^{P-1} \frac{2\pi\hbar^2}{m_n} \cdot b \cdot \delta(\underline{r} - (n \cdot \underline{a} + m \cdot \underline{b} + p \cdot \underline{c})) \tag{3.27}$$

The scattering amplitude is the Fourier transform of the scattering potential (compare 3.23):

$$\begin{aligned} A(\underline{Q}) &= \sum_{n,m,p} b \int e^{i\underline{Q}\cdot\underline{r}}\,\delta\left(\underline{r}-\left(n\cdot\underline{a}+m\cdot\underline{b}+p\cdot\underline{c}\right)\right)d^3r \\ &= b\,\underbrace{\sum_{n=0}^{N-1} e^{in\underline{Q}\cdot\underline{a}} \sum_{m=0}^{M-1} e^{im\underline{Q}\cdot\underline{b}} \sum_{p=0}^{P-1} e^{ip\underline{Q}\cdot\underline{c}}}_{\text{geometrical series}} \end{aligned} \tag{3.28}$$

Summing up the geometrical series, we obtain the scattered intensity:

$$\boxed{I(\underline{Q}) \sim \left|A(\underline{Q})\right|^2 = |b|^2 \cdot \frac{\sin^2 \frac{1}{2} N \underline{Q}\cdot\underline{a}}{\sin^2 \frac{1}{2} \underline{Q}\cdot\underline{a}} \cdot \frac{\sin^2 \frac{1}{2} M \underline{Q}\cdot\underline{b}}{\sin^2 \frac{1}{2} \underline{Q}\cdot\underline{b}} \cdot \frac{\sin^2 \frac{1}{2} P \underline{Q}\cdot\underline{c}}{\sin^2 \frac{1}{2} \underline{Q}\cdot\underline{c}}} \tag{3.29}$$

As expected, the scattered intensity is proportional to the magnitude square of the scattering length b. The dependence on the scattering vector $\underline{Q}$ is given by the so-called *Laue-function*. The latter is plotted along one lattice direction $\underline{a}$ in figure 3.5.

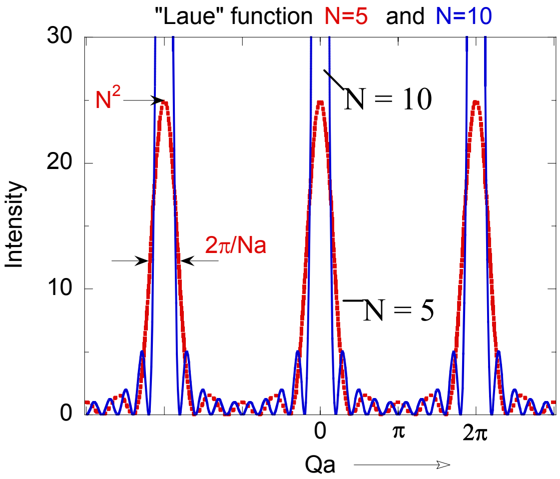

Fig. 3.5: Laue-function along the lattice direction $\underline{a}$ for a lattice with 5 and 10 periods, respectively.

The main maxima are found at the positions $Q = n \cdot \frac{2\pi}{a}$. The maximum intensity scales with the square of the number of periods, the half-width is given approximately by $\frac{2\pi}{N\cdot a}$. The more periods contribute to coherent scattering, the sharper and higher are the main peaks. Between the main peaks, there are N-2 side maxima. With increasing number of periods N, their intensity becomes rapidly negligible compared to the intensity of the main peaks. The main peaks are of course the well known *Bragg-reflections*, which we obtain when scattering from a crystal lattice. From the position of these Bragg peaks in momentum space, the metric of the unit cell can be deduced (lattice constants a, b, c and unit cell angles α, β, γ). The width of the Bragg peaks is determined by the size of the coherently scattering volume (parameters N, M and P), among other factors. Details will be given in subsequent chapters.

3.5 Coherent and Incoherent Scattering

In the last section, we assumed that we have the same interaction potential for all lattice sites. In the case of x-ray scattering, this can be well realised for a chemically clean sample, for example a Ni single crystal. However, neutrons are scattered from the nuclei and for a given atomic species, there can exist several isotopes with different scattering lengths (five different isotopes for the case of nickel). Moreover, the scattering length depends on the orientation of the nuclear spin relative to the neutron spin. In this section we will discuss the effects of these special properties of the interaction of neutrons and nuclei for the scattering from condensed matter.

Let us assume an arrangement of atoms with scattering lengths b_i on fixed positions $\underline{R}_i$. For this case, the scattering potential writes:

$$V(\underline{r}) = \frac{2\pi\hbar^2}{m_n} \sum_i b_i \delta(\underline{r} - \underline{R}_i) \tag{3.30}$$

The scattering amplitude is obtained from a Fourier transform:

$$A(\underline{Q}) = \sum_i b_i e^{i\underline{Q}\cdot\underline{R}_i} \tag{3.31}$$

When we calculate the scattering cross section, we have to take into account that the different isotopes are distributed randomly over all sites. Also the nuclear spin orientation is random, except for very low temperatures in external magnetic fields. Therefore, we have to average over the random distribution of the scattering length in the sample:

$$\frac{d\sigma}{d\Omega}(\underline{Q})=\left|A(\underline{Q})\right|^2=\left\langle \sum_i b_i \; e^{i\underline{Q}\cdot\underline{R}_i}\cdot\sum_j b_j^* e^{-i\underline{Q}\underline{R}_j}\right\rangle$$

$$\uparrow\ \text{average over the random distribution}\ \uparrow$$

$$=\sum_i\sum_j\left\langle b_i b_j^*\right\rangle e^{i\underline{Q}\left(\underline{R}_i-\underline{R}_j\right)} \qquad (3.32)$$

In calculating the expectation value of the product of the two scattering lengths at sites i and j, we have to take into account that according to the above assumption, the distribution of the scattering length on the different sites is completely uncorrelated. This implies that for i ≠ j, the expectation value of the product equals to the product of the expectation values. Only for i = j, we have a correlation, which gives an additional term describing the mean quadratic deviation from the average:

$$\left\langle b_i b_j\right\rangle=\begin{cases}\langle b\rangle\langle b\rangle=\langle b\rangle^2 & i\neq j\\ \left\langle b^2\right\rangle\underset{\uparrow}{=}\langle b\rangle^2+\left\langle\left(b-\langle b\rangle\right)^2\right\rangle & i=j\end{cases}$$

$$\left\langle\left(b-\langle b\rangle\right)^2\right\rangle=\left\langle b^2-2b\langle b\rangle+\langle b\rangle^2\right\rangle=\left\langle b^2\right\rangle-\langle b\rangle^2 \qquad (3.33)$$

Therefore, we can write the cross section in the following form:

$$\boxed{\begin{aligned}\frac{d\sigma}{d\Omega}(\underline{Q})&=\langle b\rangle^2\left|\sum_i e^{i\underline{Q}\cdot\underline{R}_i}\right|^2 &&\text{"}\mathit{coherent}\text{"}\\ &\quad+N\left\langle\left(b-\langle b\rangle\right)^2\right\rangle &&\text{"}\mathit{incoherent}\text{"}\end{aligned}} \qquad (3.34)$$

The scattering cross section is as a sum of two terms. Only the first term contains the phase factors $e^{i\underline{Q}\cdot\underline{R}}$, which result from the coherent superposition of the scattering from pairs of scatterers. This term takes into account interference effects and is therefore named *coherent scattering*. Only the scattering length averaged over the isotope- and nuclear spin- distribution enters this term. The second term in (3.34) does not contain any phase information and is proportional to the number N of atoms (and not to N^2!). This term is not due to the interference of scattering from different atoms. As we can see from (3.33) (line i = j), this term corresponds to the scattering from single atoms, which subsequently superimpose in an incoherent manner (adding intensities, not amplitudes!). This is the reason for the intensity being proportional to the number N of atoms. Therefore the second term is called *incoherent scattering*. Coherent and incoherent scattering are illustrated in figure 3.6.

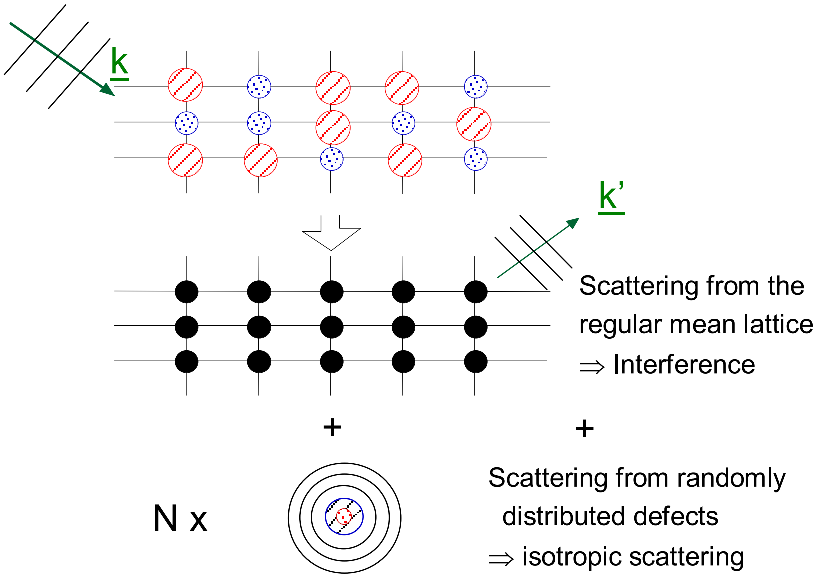

Fig. 3.6: *Two-dimensional illustration of the scattering process from a lattice of N atoms of a given chemical species, for which two isotopes (small dotted circles and large hatched circles) exist. The area of the circle represents the scattering cross section of the single isotope. The incident wave (top part of the figure for a special arrangement of the isotopes) is scattered coherently only from the average lattice. This gives rise to Bragg peaks in certain directions. In the coherent scattering only the average scattering length is visible. Besides these interference phenomena, an isotropic background is observed, which is proportional to the number N of atoms and to the mean quadratic deviation from the average scattering length. This incoherent part of the scattering is represented by the lower part of the figure.*

The most prominent example for *isotope incoherence* is elementary nickel. The scattering lengths of the nickel isotopes are listed together with their natural abundance in table 3.1 [3]. The differences in the scattering lengths for the various nickel isotopes are enormous. Some isotopes even have negative scattering lengths. This is due to resonant bound states, as compared to the usual potential scattering.

Isotope	Natural Abundance	Nuclear Spin	Scattering Length [fm]
^{58}Ni	68.27 %	0	14.4(1)
^{60}Ni	26.10 %	0	2.8(1)
^{61}Ni	1.13 %	$^{3}/_{2}$	7.60(6)
^{62}Ni	3.59 %	0	-8.7(2)
^{64}Ni	0.91 %	0	-0.37(7)
Ni			10.3(1)

Tab. 3.1: The scattering lengths of the nickel isotopes and the resulting scattering length of natural $_{28}$Ni [3].

Neglecting the less abundant isotopes ^{61}Ni and ^{64}Ni, the average scattering length is calculated as:

$$\langle b\rangle \approx \left[0.68\cdot 14.4+0.26\cdot 2.8+0.04\cdot(-8.7)\right]fm \;\approx 10.2\,fm \tag{3.35}$$

which gives the total coherent cross section of:

$$\Rightarrow \sigma_{coherent}=4\pi\langle b\rangle^{2} \;\approx 13.1\,barn\;(exact:13.3(3)barn) \tag{3.36}$$

The incoherent scattering cross section per nickel atoms is calculated from the mean quadratic deviation:

$$\begin{aligned}\sigma_{incoherent}^{Isotope} &= 4\pi\Big[0.68\cdot(14.4-10.2)^{2}+0.26\cdot(2.8-10.2)^{2}\\ &\quad +0.04\cdot(-8.7-10.2)^{2}\Big]fm^{2}\\ &\approx 5.1barn\;(exact:5.2(4)barn)\end{aligned} \tag{3.37}$$

Values in parentheses are the exact values taking into account the isotopes ^{61}Ni and ^{64}Ni and the nuclear spin incoherent scattering (see below). From (3.36) and (3.37), we learn that the incoherent scattering cross section in nickel amounts to more than one third of the coherent scattering cross section.

The most prominent example for *nuclear spin incoherent scattering* is elementary hydrogen. The nucleus of the hydrogen atom, the proton, has the nuclear spin I = ½. The total nuclear spin of the system H + n can therefore adopt two values: J = 0 and J = 1. Each state has its own scattering length: b_- for the singlett state (J = 0) and b_+ for the triplett state (J = 1) - compare table 3.2.

Total Spin	Scattering Length	Abundance
J = 0	$b_- = - 47.5$ fm	$\frac{1}{4}$
J = 1	$b_+ = 10.85$ fm	$\frac{3}{4}$
<b> = - 3.739(1) fm		

Tab. 3.2: Scattering lengths for hydrogen [3].

As in the case of isotope incoherence, the average scattering length can be calculated:

$$\langle b\rangle = \left[\frac{1}{4}(-47.5) + \frac{3}{4}\cdot(10.85)\right] fm \;= -3.74\, fm \tag{3.38}$$

This corresponds to a coherent scattering cross section of about ≈ 1.76 barn [3]:

$$\Rightarrow \sigma_{coherent} = 4\pi\langle b\rangle^2 = 1.7568(10)\, barn \tag{3.39}$$

The nuclear spin incoherent part is again given by the mean quadratic deviation from the average:

$$\sigma_{incoherent}^{nuclear\ spin} = 4\pi\left[\frac{1}{4}(-47.5+3.74)^2 + \frac{3}{4}(10.85+3.74)^2\right] fm^2 = 80.2\, barn$$

$$(\textit{exact: } 80.26(6)\ barn) \tag{3.40}$$

Comparing (3.39) and (3.40), it is immediately clear that hydrogen scatters mainly incoherently. As a result, we observe a large background for all samples containing hydrogen.

We note immediately that we should avoid all organic glue for fixing our samples to a sample stick. Finally, we note that deuterium with nuclear spin I = 1 has a much more favourable ratio between coherent and incoherent scattering:

$$\sigma_{coh.}^{D} = 5.592(7) barn; \quad \sigma_{inc.}^{D} = 2.05(3) barn \tag{3.41}$$

The coherent scattering lengths of hydrogen (-3.74 fm) and deuterium (6.67 fm) are significantly different. This can be used for contrast variation by isotope substitution in all samples containing hydrogen, i. e. in biological samples or soft condensed matter samples, see corresponding chapters.

A further important element, which shows strong nuclear incoherent scattering, is vanadium. Natural vanadium consists to 99,75 % of the isotope ^{51}V with nuclear spin 7/2. By chance, the ratio between the scattering lengths b_+ and b_- of this isotope are approximately equal to the reciprocal ratio of the abundances. Therefore, the coherent scattering cross section is negligible and the incoherent cross section dominates [3]:

$$\sigma_{coh}^{V} = 0.01838(12)\, barn; \quad \sigma_{incoh}^{V} = 5.08(6)\, barn \tag{3.42}$$

For this reason, Bragg scattering of vanadium is difficult to observe above the large incoherent background. However, since incoherent scattering is isotropic, the scattering from vanadium can be used to calibrate multi-detector arrangements.

Here, we will not discuss scattering lengths for further elements and refer to the values tabulated in [3].

3.6 Magnetic Neutron Scattering

So far, we have only discussed the scattering of neutrons by the atomic nuclei. Apart from nuclear scattering, the next important process is the scattering of neutrons by the magnetic moments of unpaired electrons. This so-called magnetic neutron scattering comes about by the magnetic dipole-dipole interaction between the magnetic dipole moment of the neutron and the magnetic field of the unpaired electrons, which has spin and orbital angular momentum contributions (see figure 3.7).

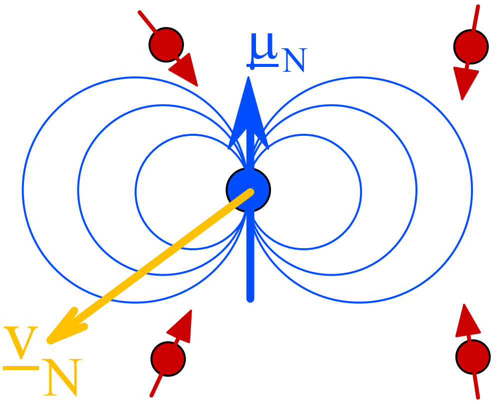

Fig. 3.7: Schematic illustration of the interaction process of a neutron with the atomic magnetic moments via the dipole interaction.

This magnetic neutron scattering allows us to study the magnetic properties of a sample on an atomic level, i. e. with atomic spatial- and atomic energy- resolution. A typical problem studied is the determination of a magnetic structure, i. e. the magnitudes and arrangements of the magnetic moments within the sample. Besides the well-known and simple ferromagnets, for which all moments are parallel, there exists a whole zoo of complicated ferri- and antiferromagnetic structures, such as helical structures, spin density waves, etc. (compare figure 3.8).

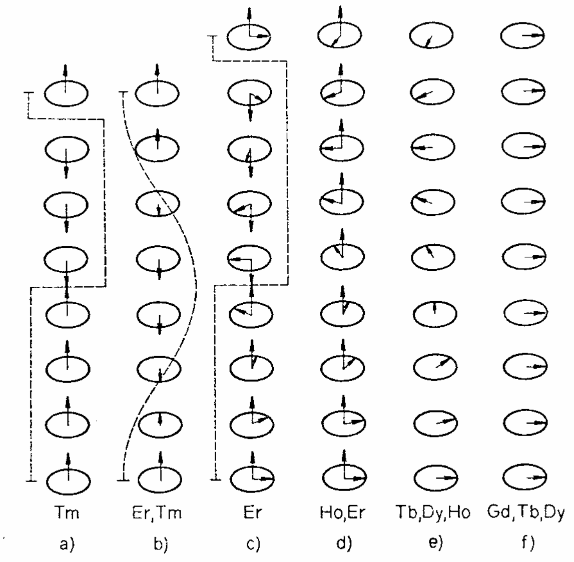

Fig. 3.8: Schematic illustration of the magnetic structures of the hexagonal rare earth metals. Within the hexagonal basal plane, all moments are parallel. The figure shows the sequence of moments in successive planes along the hexagonal c-axis. Besides simple ferromagnetic phases (f), helical (e), conical (d) and c-axis-modulated structures (b) etc. are observed.

These magnetic structures can be understood on the basis of magnetic interactions, which again can be determined by neutron scattering from measurements of the magnetic excitation spectra. Magnetic structures are only stable in a certain range of theromdynamic parameters, such as temperature, pressure or magnetic field. As we approach the limits of a stability region, magnetic phase transitions into a different magnetic phase occur. An example is the transition from a long-range magnetic order at low temperatures to a paramagnetic high temperature phase. By means of neutron scattering, the spectra of magnetisation fluctuations close to a magnetic phase transition can be determined. Such measurements provide the experimental foundation of the famous renormalisation group theory of phase transitions.

In what follows, we will give an introduction into the formalism of magnetic neutron scattering. Again, we will restrict ourselves to the case of elastic magnetic scattering. Examples for magnetic scattering will we given in a later chapter.

To derive the magnetic scattering cross section of thermal neutrons, we consider the situation shown in figure 3.9: a neutron with the nuclear moment μ_N is at position $\underline{R}$ with respect to an electron with spin $\underline{S}$, moving with a velocity $\underline{v}_e$.

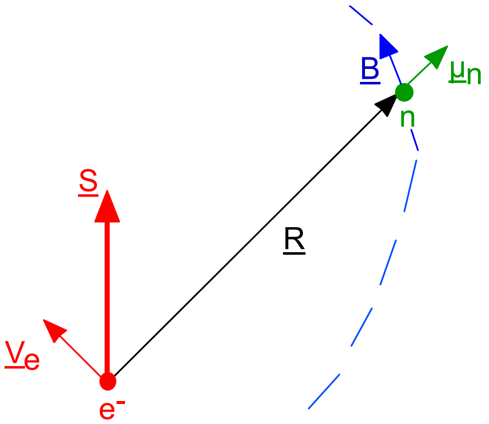

Fig. 3.9: Geometry for the derivation of the interaction between neutron and electron.

Due to its magnetic dipole moment, the neutron interacts with the magnetic field of the electron according to:

$$\mathbf{V}_m = -\underline{\mu}_n \cdot \underline{B} \tag{3.43}$$

Here, the magnetic moment of the neutron is given by:

$$\underline{\mu}_n = -\gamma_n \mu_N \cdot \underline{\sigma} \tag{3.44}$$

$\underline{\sigma}$ denotes the spin operator, μ_N the nuclear magneton and γ_N = -1.913 the gyromagnetic factor of the neutron. The magnetic field $\underline{B}$ of an electron is due to a spin- and orbital- part $\underline{B} = \underline{B}_S + \underline{B}_L$. The dipole field of the spin moment is given by:

$$\underline{B}_S = \underline{\nabla} \times \left(\frac{\underline{\mu}_e x \underline{R}}{R^3} \right) \quad ; \quad \underline{\mu}_e = -2\mu_B \cdot \underline{S} \tag{3.45}$$

The field due to the movement of the electron is given according to Biot-Savart:

$$\underline{B}_L = \frac{-e}{c} \frac{\underline{v}_e \times \underline{R}}{R^3} \tag{3.46}$$

The magnetic scattering cross section for a process, where the neutron changes its wave vector from $\underline{k}$ to $\underline{k}'$ and the projection of its spin moment to a quantisation axis z from σ_z to σ_z' can be expressed within the first Born approximation:

$$\frac{d\sigma}{d\Omega} = \left(\frac{m_n}{2\pi\hbar^2} \right)^2 \left| \left\langle \underline{k}' \sigma_z' \middle| \mathbf{V}_m \middle| \underline{k} \sigma_z \right\rangle \right|^2 \tag{3.47}$$

As mentioned, we only consider the single differential cross section for elastic scattering. Introducing the interaction potential from (3.43) to (3.46) in (3.47), we obtain after a lot of algebra [4, 5]:

$$\frac{d\sigma}{d\Omega} = (\gamma_n r_0)^2 \left| -\frac{1}{2\mu_B} \left\langle \sigma_z' \middle| \underline{\sigma} \cdot \underline{M}_\perp (\underline{Q}) \middle| \sigma_z \right\rangle \right|^2 \tag{3.48}$$

The pre-factor $\gamma_n r_0$ has the value $\gamma_n r_0 = 0.539 \cdot 10^{-12}$ cm = 5.39 fm. Here, $\underline{M}_\perp(\underline{Q})$ denotes the component of the Fourier transform of the sample magnetisation, which is perpendicular to the scattering vector $\underline{Q}$:

$$\underline{M}_{\perp}(\underline{Q}) = \hat{\underline{Q}} \times \underline{M}(\underline{Q}) \times \hat{\underline{Q}} \tag{3.49}$$

$$\underline{M}(\underline{Q}) = \int \underline{M}(\underline{r}) e^{i\underline{Q}\cdot\underline{r}} d^3 r \tag{3.50}$$

The total magnetisation is given as a sum of the spin- and orbital-angular- momentum part according to:

$$\begin{aligned} &\underline{M}(\underline{r}) = \underline{M}_S(\underline{r}) + \underline{M}_L(\underline{r}) \\ &\underline{M}_S(\underline{r}) = -2\mu_B \cdot \underline{S}(\underline{r}) = -2\mu_B \sum_i \delta(\underline{r} - \underline{r}_i)\underline{S}_i \end{aligned} \tag{3.51}$$

(3.48) tells us that with magnetic neutron scattering, we are able to determine the magnetisation $\underline{M}(\underline{r})$ in microscopic atomic spatial co-ordinates $\underline{r}$. This gives a lot more information as a simple macroscopic measurement, where we obtain the ensemble average of the magnetisation over the entire sample. We also see from (3.48) that the orientation of the nuclear spin momentum of the neutron (represented by σ_z) plays an important role in magnetic scattering. This is not surprising, since magnetism is a vector property of the sample and obviously there should be an interaction with the vector property of the neutron, its nuclear magnetic moment. Therefore, the analysis of the change of the direction of the neutron nuclear moment in the scattering process should give us valuable additional information as compared to a determination of the change of energy and momentum direction of the neutron alone. These so-called polarisation analysis experiments are discussed in the following chapter. For our present purposes, we will completely neglect these dependencies. Finally, to obtain an idea of the size of magnetic scattering relative to nuclear scattering, we can replace the matrix element in (3.48) for a spin ½ particle by the value 1 μ_B. This gives us an "equivalent" scattering length for magnetic scattering of 2.696 fm for a spin ½ particle. This value corresponds quite well to the scattering length of cobalt, which means that magnetic scattering is comparable in magnitude to nuclear scattering.

In contrast to nuclear scattering, we obtain for magnetic scattering a directional term: neutrons only "see" the component of the magnetisation perpendicular to the scattering vector (see figure 3.10).

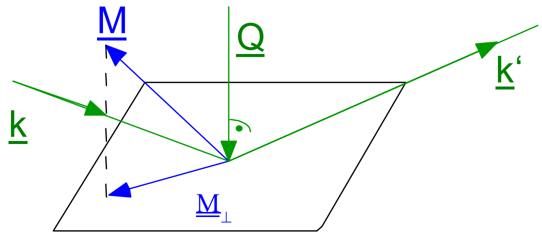

Fig. 3.10: For magnetic neutron scattering, only the component $\underline{M}_\perp$ of the magnetisation perpendicular to the scattering vector $\underline{Q}$ is of relevance.

That only $\underline{M}_\perp$ gives rise to magnetic neutron scattering, can be understood from the notion that neutrons are scattered from the dipolar field of the electrons. This is depicted for two different geometries in figure 3.11. For the case that the magnetisation is parallel to the scattering vector, the planes for equal phase factor cut though the dipolar field in such a way that due to symmetry reasons, the field averaged over these planes vanishes. This is no longer the case, if the magnetisation is perpendicular to the scattering vector. This special directional dependence allows it to determine the orientation of magnetic moments relative to the lattice.

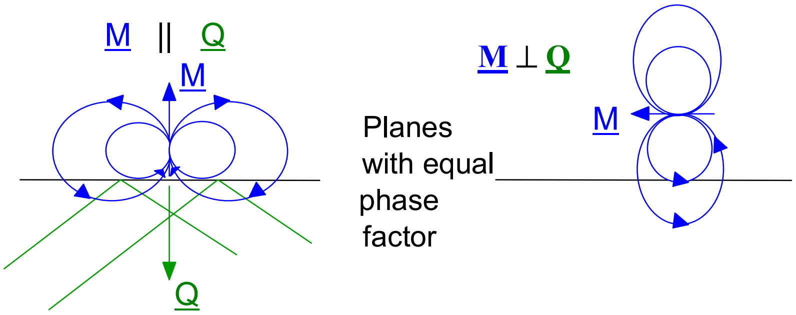

Fig. 3.11: Illustration of the directional dependence for the scattering from a dipolar field: in the case where $\underline{M} \parallel \underline{Q}$ the dipolar field averaged over planes with equal phase factors is zero, so that no magnetic scattering appears.

A second speciality of magnetic scattering as compared to nuclear scattering is the existence of the so-called *form factor*. The form factor describes the fact that the scattering amplitude drops with increasing momentum transfer. This occurs because the object, from which we scatter, namely the electron cloud of an atom, has a size comparable to the wave length of thermal neutrons. Since the distribution of the magnetic field for spin and orbital angular momentum is completely different (compare figure 3.12 for the case of a classical Bohr orbit), different Q-dependencies of the corresponding form factors result (compare figure 3.13).

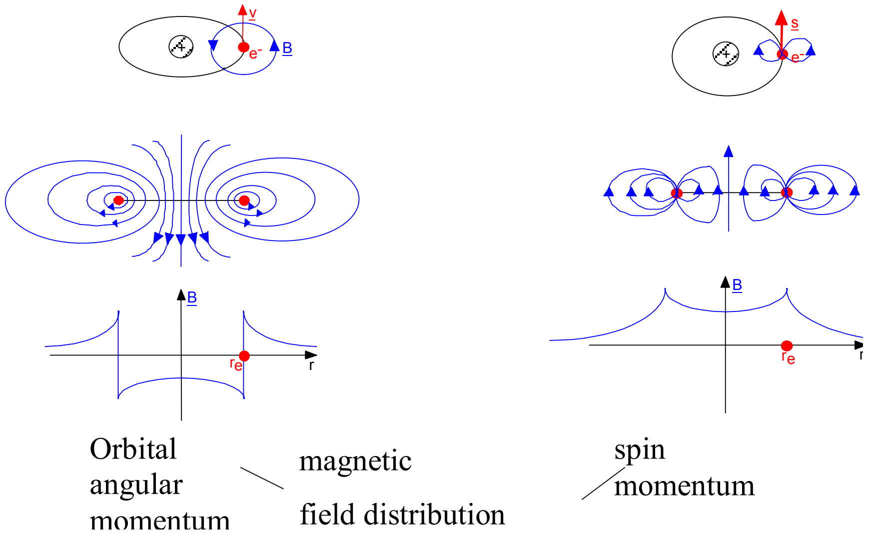

Fig. 3.12: Schematic illustration of the magnetic field distribution due to spin - (S) and orbital- (L) angular momentum in the case of a Bohr orbit. The magnetic field due to the spin moment is much more spread out than the one due to the orbital angular momentum.

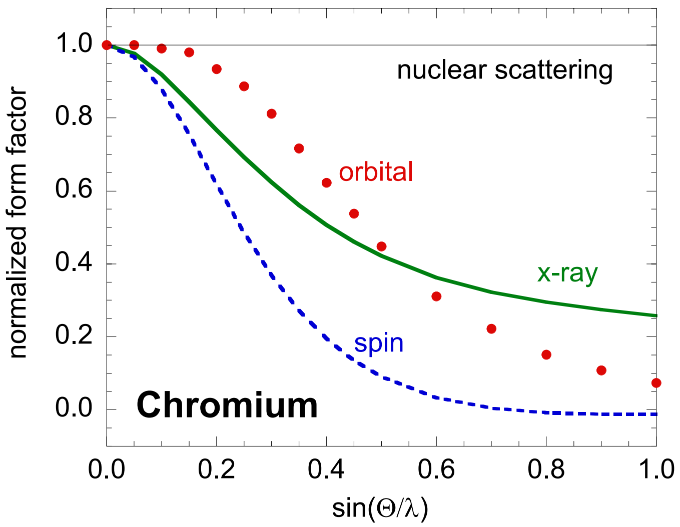

Fig. 3.12: Form-factor of Cr [7, 8]. Due to the different distribution of the magnetic field for S and L according to figure 3.11, a more rapid decrease of the scattering amplitude as a function of momentum transfer results for the spin momentum. For the x-ray form factor, the inner electrons play an important role, too. Therefore, the x-ray form factor drops slower as compared to the magnetic form factor. Finally, on the Å length scale of the thermal neutron wave length, the nucleus is point-like. Therefore, nuclear scattering is independent of the momentum transfer.

Since the scattering amplitude is proportional to a Fourier transform of the scattering power density in direct space, the scattering amplitude decreases faster with momentum transfer if the scattering occurs from a larger object in direct space. Since the unpaired magnetic electrons are located in the outermost electronic shells, the magnetic form factor drops faster than the x-ray form factor. Compared to the natural length scale of the neutron wave length, the nucleus is point-like, which results in a scattering amplitude being independent of momentum transfer. Finally, we want to mention that the magnetic form factor can in general be anisotropic, if the magnetisation density distribution is anisotropic.

How the form factor comes about is most easily understood in the simple case of pure spin scattering, i. e. for atoms with spherical symmetric (L = 0) ground state, such as Mn^{2+} or Fe^{3+}. Moreover, the derivation is simplified for ionic crystals, where the electrons are located around an atom. In figure 3.13 we define the relevant quantities for a derivation.

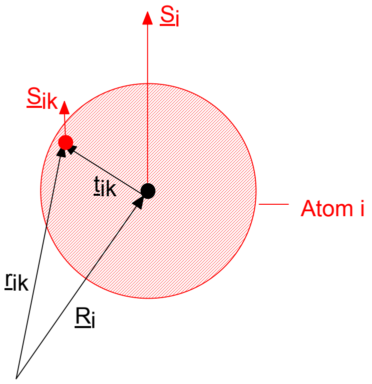

Fig. 3.13: Definition of the relevant quantities for a derivation of the spin-only form factor.

We denote the spin operators of the electrons of atom i with $\underline{s}_{ik}$. The spatial co-ordinates of the electron number k in atom i are $\underline{r}_{ik} = \underline{R}_i + \underline{t}_{ik}$, where $\underline{R}_i$ denotes the position vector to the nucleus of atom i. Now we proceed to separate the intra-atomic quantities. We can write the operator for the magnetisation density as:

$$\underline{M}_S(\underline{r}) = -2\mu_B \sum_{ik} \delta(\underline{r} - \underline{r}_{ik}) \cdot \underline{s}_{ik} \tag{3.52}$$

The Fourier transform of this magnetisation density is calculated to:

$$\underline{M}(\underline{Q}) = \int \underline{M}_S(\underline{r}) e^{i\underline{Q}\cdot\underline{r}} d^3r = \sum_{ik} e^{i\underline{Q}\cdot\underline{r}_i} \underline{s}_{ik} = \sum_i e^{i\underline{Q}\cdot\underline{R}_i} \sum_k e^{i\underline{Q}\cdot\underline{t}_{ik}} \cdot \underline{s}_{ik} \quad (3.53)$$

To calculate the scattering cross section, we now have to determine the expectation value of this operator for the quantum mechanical state of the sample averaged over the thermodynamic ensemble. This leads to

$$\underline{M}(\underline{Q}) = -2\mu_B \cdot f_m(\underline{Q}) \cdot \sum e^{i\underline{Q}\cdot\underline{R}_i} \cdot \underline{S}_i \quad (3.54)$$

The single differential cross section for elastic scattering is thus given by:

$$\frac{d\sigma}{d\Omega} = (\gamma_n r_0)^2 \left| f_m(\underline{Q}) \sum_i S_{i\perp} e^{i\underline{Q}\underline{R}_i} \right|^2 \quad (3.55)$$

Here, $f_m(\underline{Q})$ denotes the form factor, which is connected with the spin density of the atom via a Fourier transform:

$$f_m(\underline{Q}) = \int_{Atom} \rho_s(\underline{r}) e^{i\underline{Q}\cdot\underline{r}} d^3r \quad (3.56)$$

With the form (3.55), we have expressed the cross section in simple atomic quantities, such as the expectation values of the spin moment at the various atoms. The distribution of the spin density within an atom is reflected in the magnetic form factor (3.56).

For ions with spin and orbital angular momentum, the cross section takes a significantly more complicated form [4, 5]. Under the assumption that spin- and orbital- angular momentum of each atom couple to the total angular momentum $\underline{J}_i$ (L/S-coupling) and for rather small momentum transfers (the reciprocal magnitude of the scattering vector has to be small compared to the size of the electron orbits), we can give a simple expression for this cross section in the so-called *dipole approximation*:

$$\frac{d\sigma}{d\Omega} = (\gamma_n r_o)^2 \cdot \left| \frac{g_J}{2} f_m(Q) \sum_i J_{i\perp} e^{i\underline{Q}\cdot\underline{R}_i} \right|^2 \quad (3.57)$$

Here the magnetic form factor writes:

$$f_m(Q) = \langle j_o(Q) \rangle + C_2 \langle j_2(Q) \rangle \tag{3.58}$$

g_J denotes the Lande g-factor, $C_2 = \frac{2}{g_J}$ -1 and

$$\langle j_l(Q) \rangle = 4\pi \int_0^\infty j_l(Qr) R^2(r) r^2 dr \tag{3.59}$$

are the spherical transforms of the radial density distributions R(r) with the spherical Bessel functions $j_l(Qr)$. For isolated atoms, the radial part R(r) has been determined by Hartree-Fock-calculations and the functions $\langle j_0(Q) \rangle$ and $\langle j_2(Q) \rangle$ in (3.58) have been tabulated [6].

After having introduced the principles of magnetic scattering, we will discuss applications in chapter 16.

References

[1] J. M. Cowley "Diffraction Physics" North-Holland, Amsterdam 1990

[2] B. W. Batterman, H. Cole "Dynamical Diffraction of X Rays by Perfect Crystals", Reviews of Modern Physics 36, 3, 681 - 717 (1964)

[3] V. F. Sears "Neutron Scattering Length and Cross Sections", Neutron News 3 (1992), 26 - 37

[4] G. L. Squires "Introduction to the theory of thermal neutron scattering" Cambridge University Press, Cambridge (1978)

[5] S. W. Lovesey "Theory of neutron scattering from condensed matter" Volume 2: Polarisation effects and magnetic scattering, Clarendon Press, Oxford (1987)

[6] A. J. Freeman & R. E. Watson, Acta Cryst. 14 (1961), 231

[7] J. Strempfer, Th. Brückel et al Eur. Phys. J. B14 (2000), 63

[8] J. Strempfer, Th. Brückel et al Physica B 267-268 (1999), 56